
SEMICONDUCTOR STRUCTURES, INTERFACES, AND SURFACES

Simulation of Interaction Between Nickel and Silicon Carbide during the Formation of Ohmic Contacts

O. V. Aleksandrov^a and V. V. Kozlovski^b

^aSt. Petersburg State Electrotechnical University “LÉTI,” St. Petersburg, 197376 Russia

^ae-mail: Aleksandr_ov@mail.ru

^bSt. Petersburg State Polytechnical University, St. Petersburg, 195251 Russia

^be-mail: Kozlovski@tuexph.stu.neva.ru

Submitted November 6, 2008; accepted for publication November 17, 2008

Abstract—For the first time, the quantitative model of interaction between silicide-forming metal Ni and single-crystalline SiC is developed on the basis of the mutual diffusion of components and the volume silicide-formation reaction. The model makes it possible to describe satisfactorily the basic properties of the redistribution of components during the thermal annealing and during the proton irradiation of the Ni–SiC system at elevated temperatures, specifically: the presence of an extended reaction zone, an excess of the carbon concentration over the silicon concentration at the interface with the SiC substrate, and the carbon accumulation near the surface. It is shown that the stimulation of the interaction between metal Ni and SiC by the proton irradiation at an elevated temperature occurs due to an increase in the metal diffusivity and in the constants of rates of reactions of solid-phase silicide-formation. An acceleration of metal diffusion is associated with the generation of elementary radiation defects (interstitial atoms and vacancies), while an increase in the constants of rates of solid-phase reactions is attributed to a generation of vacancies, which contribute free volume.

PACS numbers: 61.80.Jh, 68.35.Dv, 68.35.Fx, 68.55.Jk, 68.55.Nq, 73.40.Cg

DOI: 10.1134/S1063782609070100

1. INTRODUCTION

The interest in the processes of metal–semiconductor interaction at the interphase boundary is caused substantially by the necessity of formation of both rectifying and ohmic contacts in modern semiconductor devices. The special difficulties are observed when fabricating the ohmic contacts to wide-gap semiconductors, in particular, to silicon carbide (see reviews [1, 2]). For the formation of contacts to SiC, these are the chemical reactions of interaction of metal atoms either with silicon atoms (the silicide formation with Ni, Pd, Pt, and Co metals) or with carbon atoms (the formation of carbides with Ti, Ta, Cr, and Zr metals) that play the determining role. We consider the case of formation of ohmic contact to *n*-SiC with the help of the most widely used silicide-forming metal nickel. The Ni–SiC contact becomes ohmic (nonrectifying) at the annealing temperatures above 900°C [1, 2]. At these temperatures, the Ni film interacts with SiC with the formation of nickel silicides: Ni₃Si, Ni₂Si, NiSi, and NiSi₂, from which the silicide Ni₂Si enriched with metal prevails [3–6]. In the reaction, the reduction of carbon takes place. Carbon is found in the state of elementary graphite, which is either uniformly distributed over the silicide thickness [1, 4, 5, 7, 8] or accumulates at the internal interface of the silicide–SiC substrate [9, 10] and near the sili-

cide surface [2, 6, 11–13] in the form of a layer [6, 10, 12, 13] or nanodimensional clusters [1, 7, 11].

The phase-formation processes in the Ni–SiC system appreciably define the electrical and structural characteristics of the contact. The formation of an ohmic contact first was associated with the formation of silicide Ni₂Si [1, 2]. However, it was shown that the Ni₂Si phase together with the Ni₃Si phase, which is more enriched with metal, is formed already at temperatures $T = 500\text{--}600^\circ\text{C}$ [3, 4, 6–8], when the Ni–*n*-SiC contact has the rectifying characteristic of the Schottky diode [1, 7]. In [12, 13], the formation of the Ni–SiC ohmic contact is related to the outward diffusion of carbon released in the SiC dissociation. It was assumed that the carbon vacancies having a donor level in SiC and, consequently, reducing the Schottky-barrier height are formed in this case. It seems that the results of experiments [10] with selective etching off of the Ni₂Si film as well as the graphite layer from the ohmic contact formed at high-temperature ($T = 1040^\circ\text{C}$) annealing of the Ni–SiC structures testify in favor of this assumption. In both cases, the contact’s ohmic property was retained, from which the authors of [10] concluded that the physical properties of the near-contact SiC layer varied, probably, due to forming the carbon vacancies. However, the capacitance-spectroscopy method [7, 14] revealed no level related

to the carbon vacancies after the annealing of the Ni–SiC contact at the temperature of $T = 950^\circ\text{C}$.

It is known that the topochemical reactions set in the region of extended crystal-lattice defects (dislocations, grain boundaries, etc.), where the energy losses on the bond deformation are minimal, there is certain free volume facilitating the reorientation of reacting particles. Therefore, such reactions are very sensitive to all damages in structure facilitating the formation of new-phase nuclei including those related to the radiation effects increasing the defect concentration. An irradiation of the Ni–SiC contact with Ar ions [15] and protons [16, 17] makes it possible to decrease the temperature of formation of ohmic contacts to 600–800°C. The effect was associated with increasing the diffusivity of nickel [15] or silicon [17] atoms due to increasing the concentration of intrinsic point defects formed during the irradiation or the subsequent annealing. We note that the proton irradiation at higher temperatures stimulates the formation of silicide phases of nickel monosilicide and disilicide (NiSi and NiSi_2), which are more enriched with silicon than the Ni_2Si phase prevailing in the case of usual thermal annealing [17].

Both under the thermal annealing and under the proton irradiation, the distribution of the components of interaction between Ni and SiC has a number of features. First, the depth distribution of components is not limited only to the phase boundary and has a relatively extended character [9, 11, 13, 16, 17] that is indicative of the volume nature of proceeding reactions. Second, the carbon accumulation both near the sample surface [2, 6, 11–13, 16, 17] and near the interface with the SiC substrate [9, 10, 16, 17] is observed.

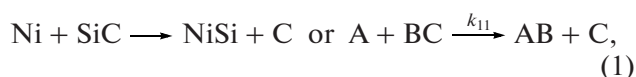
The simplest model of the metal–semiconductor interaction consists in the mutual diffusion of the metal into the semiconductor and the semiconductor components into the metal. A difference between the diffusivities of atoms migrating in the opposite directions results in the occurrence of the Kirkendall effect [18]. The mutual diffusion and the interphase-boundary displacement in the diffusion pair forming a continuous solid solution are described in the Darken theory [19]; however, the problem of the applicability of the Darken theory to multicomponent systems with the formation of new phases remains open.

The purpose of this study is to develop the quantitative model of interaction of Ni with single-crystalline SiC on the basis of the mutual diffusion of components and the volume silicide-formation reactions.

2. MODEL DESCRIPTION

In the proposed model, we assume that, in the Ni–SiC pair, the metal interacts only with silicon forming silicides. This chemical interaction is the principal cause, which damages the rigid silicon-carbide lattice. In contrast to the Ni–Si contact, where

the formed silicides are concentrated only at the interphase boundary [20], the components of the Ni–SiC interaction are distributed within a relatively extended zone whose thickness is on the order of the initial metal-film thickness [9, 11, 13, 16, 17]. The large extent of this reaction zone is indicative of a relatively low rate of the solid-phase reaction in comparison with that of the diffusion of mobile components, which is likely caused by relatively strong Si–C chemical bonds in silicon carbide. Instead of the epitaxial growth on the phase boundary, the silicide formation proceeds here by the so-called interstitial mechanism [20, 21], in which case the fast diffusing interstitial atoms of metal assist in weakening and breaking the neighboring covalent bonds of the semiconductor, Si–C in our case, and in their replacement by silicon–metal bonds. Simultaneously, the reduction of carbon in the elemental form takes place, and it does not interact with the metal. The reaction of the metal-monosilicide formation by an example of Ni has the form



where A is nickel, B is silicon, and C is carbon. At relatively low annealing temperatures ($T = 600\text{--}950^\circ\text{C}$), the metal-enriched silicide (Ni_2Si) [3–5, 7, 8] is formed:



At higher temperatures ($T = 950\text{--}1100^\circ\text{C}$) [5, 11] and under proton irradiation [17], it is nickel disilicide with liberation of carbon that is formed alongside with monosilicide in the reaction



Here, k_{11} , k_{21} , and k_{12} are the rate constants for reactions (1), (2), and (3), respectively. All these reactions proceed in the SiC bulk as a result of the diffusion penetration of Ni into SiC. The metal atoms and, probably, released C atoms are the mobile components in reactions (1)–(3). For the relation $D_A \gg D_C$ between the diffusivities of metal (D_A) and carbon (D_C), we have a displacement of the interphase boundary to the surface due to the Kirkendall effect [18]. In the binary system with unlimited solubility, the mutual diffusion or the diffusion mixing of components is described by an effective heterodiffusion coefficient according to the Darken theory [19]. We assume that the diffusion mixing of Ni, Si (in the SiC composition), and reduced C also can be described in the metal–SiC system by the effective heterodiffusion coefficient (D^*). We take into account the formation of new silicide phases using the kinetic (reaction) terms in the corresponding diffusion equations. The diffusion–reaction

equations for the components of reactions (1)–(4) in the metal–SiC system has the form

$$\frac{\partial C_A}{\partial t} = \frac{\partial}{\partial x} \left(D^* \frac{\partial C_A}{\partial x} \right) - k_{11} C_A C_{BC} - k_{21} C_A C_{AB}, \quad (4)$$

$$\frac{\partial C_{BC}}{\partial t} = \frac{\partial}{\partial x} \left(D^* \frac{\partial C_{BC}}{\partial x} \right) - k_{11} C_A C_{BC} - k_{12} C_{AB} C_{BC}, \quad (5)$$

$$\frac{\partial C_C}{\partial t} = \frac{\partial}{\partial x} \left(D^* \frac{\partial C_C}{\partial x} \right) + k_{11} C_A C_{BC} + k_{12} C_{AB} C_{BC}, \quad (6)$$

$$\frac{\partial C_{AB}}{\partial t} = k_{11} C_A C_{BC} - k_{21} C_A C_{AB}, \quad (7)$$

$$\frac{\partial C_{ABB}}{\partial t} = k_{12} C_{AB} C_{BC}, \quad (8)$$

$$\frac{\partial C_{AAB}}{\partial t} = k_{21} C_A C_{AB}, \quad (9)$$

where t is the time; x is the depth; and C_A , C_{BC} , C_{AB} , C_{ABB} , C_{AAB} , and C_C are the concentrations of metal (Ni), silicon in SiC composition, metal silicide (NiSi), metal disilicide (NiSi₂), metal-enriched silicide (Ni₂Si), and free carbon, respectively. The effective heterodiffusion coefficient has the following form in our case:

$$D^* = \frac{D_A(C_{BC} + C_C + C_{AB} + C_{ABB} + C_{AAB}) + D_C C_A}{C_\Sigma}, \quad (10)$$

Here, C_Σ is the total concentration of all components, $C_\Sigma = C_A + C_{BC} + C_C + C_{AB} + C_{ABB} + C_{AAB}$. In [22, 23], it was shown that Ni is the dominant mobile component, while carbon released in the interaction of Ni with SiC is almost immobile. Therefore, we set $D_C = 0$ in Eq. (10). The metal diffusivity in various phases is different; we assume that it linearly depends on composition:

$$D_A = \frac{D_{AA} C_A + D_{AB} C_{AB} + D_{ABB} C_{ABB} + D_{AAB} C_{AAB} + D_{BC} C_{BC}}{C_A + C_{AB} + C_{ABB} + C_{AAB} + C_{BC}}, \quad (11)$$

where D_{AA} , D_{AB} , D_{ABB} , D_{AAB} , and D_{BC} are the partial diffusivities of metal in the phases of metal, monosilicide, disilicide, metal-enriched silicide, and SiC, respectively. The absence of diffusion terms in Eqs. (7)–(9) is caused by the fact that the plastic flow of material of silicides to the external surface due to the nickel-atom flux is compensated in the steady-state mode by the growth of silicide-phase flow in an opposite direction (the Kirkendall effect).

The initial conditions for Eqs. (4)–(9) are

$$C_A(x, 0) = N_{SA} \text{ for } 0 \leq x \leq h, \quad (12)$$

$$C_B(x, 0) = N_{SB} \text{ for } h \leq x \leq L, \quad (13)$$

$$\begin{aligned} C_{AB}(x, 0) &= C_{ABB}(x, 0) = C_{AAB}(x, 0) \\ &= C_C(x, 0) = 0 \text{ for all } 0 \leq x \leq L, \end{aligned} \quad (14)$$

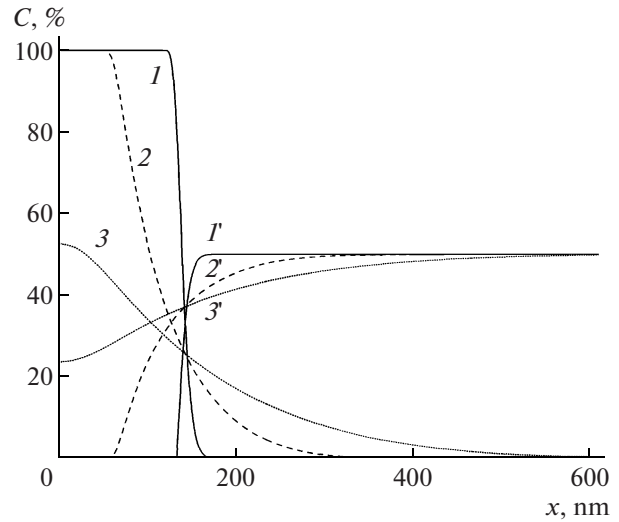


Fig. 1. Depth distribution of relative concentrations C of (1–3) metal and (1'–3') silicon (in the SiC composition) for $k_{11} = k_{21} = k_{12} = 0$. The calculation for $D_A = 6 \times 10^{-14} \text{ cm}^2/\text{s}$. The annealing time, min: 1, 1'—0.1; 2, 2'—10; 3, and 3'—60.

where h is the metal-film thickness, L is the SiC-substrate thickness (the solution-region depth), N_{SA} is the intrinsic metal-atom concentration ($N_{SA} = 9 \times 10^{22} \text{ cm}^{-3}$ for Ni), and N_{SB} is the intrinsic silicon-atom concentration in the substrate ($N_{SB} = 4.8 \times 10^{22} \text{ cm}^{-3}$ for SiC). The boundary conditions correspond to the reflecting boundaries:

$$\begin{aligned} \frac{\partial C_A}{\partial x} &= \frac{\partial C_{BC}}{\partial x} = \frac{\partial C_C}{\partial x} = 0 \\ \text{for } x &= 0 \text{ and } x = L. \end{aligned} \quad (15)$$

The set of Eqs. (4)–(9) with concentration-dependent effective heterodiffusion coefficients (10), (11), initial conditions (12)–(14), and boundary conditions (15) was solved numerically using the implicit difference scheme for Eqs. (4)–(6) and the Euler method for Eqs. (7)–(9). The parameters of the model were the metal diffusivity and the reaction-rate constants.

3. RESULTS OF CALCULATION AND COMPARISON WITH EXPERIMENT

In the metal–substrate diffusion pair with mobile metal atoms, the metal diffuses from the deposited film into the SiC substrate. As a result of the counter flow of vacancies and their subsequent annihilation at drains, there is the diffusion mixing of two materials as it is shown in Fig. 1 for no silicide formation ($k_{11} = k_{21} = k_{12} = 0$). The interphase boundary or the plane of equal relative metal and silicon concentrations (the Kirkendall plane) shifts in this case to the surface according to the Kirkendall effect [18]. The redistri-

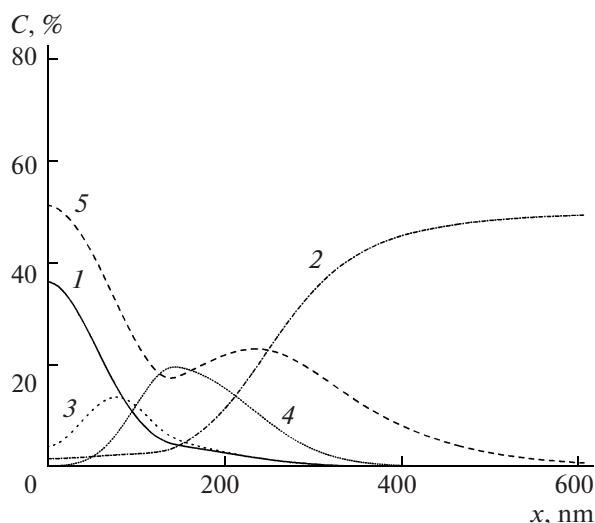


Fig. 2. Depth distribution of relative concentrations C of components for $k_{11} = k_{12} \neq 0$: 1—Ni, 2—Si (in the SiC composition), 3—NiSi, 4—NiSi₂, and 5—C. The calculation for $D_A = 6 \times 10^{-14}$ cm²/s and $k_{11} = k_{12} = 6 \times 10^{-26}$ cm³/s. The annealing time is 60 min.

bution of metal (curves 1–3) and the substrate material (silicon) in the SiC composition (curves 1'–3') is described by Eqs. (4) and (5) with the same effective heterodiffusion coefficient D^* (10) according to the Darken theory [19]. The distributions of metal and silicon concentrations become approximately symmetric to each other relative to the Kirkendall plane (see Fig. 1), while silicon remains bonded in the SiC structure and does not diffuse.

During the formation of silicide phases (for example, monosilicide NiSi and disilicide NiSi₂ for $k_{11} = k_{12} \neq 0$, $k_{21} = 0$), a transition region (reaction zone) (Fig. 2) is formed between the metal layer and the substrate. In this region, the initial phases of metal (curve 1) and SiC substrate (curve 2) coexist with new phases, i.e., the products of reactions (1) and (3) NiSi (curve 3) and NiSi₂ (curve 4). During the formation of silicide, elementary carbon is released (curve 5) and accumulates in the front part of the reaction zone adjoining to the SiC substrate and is also pushed off by a growing silicide phase to the surface and the back part of the reaction zone.

With time (Fig. 3), the integrated metal concentration in the deposited layer decreases, and the silicide concentration grows, which results in modifying the profiles of the total concentrations of metal ($C_{AS} = C_A + C_{AB} + C_{ABB}$, curves 1, 1'), silicon ($C_{BS} = C_{BC} + C_{AB} + 2C_{ABB}$, curves 2, 2'), and carbon ($C_{CS} = C_C + C_{BC}$, curves 3, 3'). The reaction zone becomes more extended shifting simultaneously both deep into the substrate and to the surface. The similar effect is observed with increasing the metal diffusivity D_A .

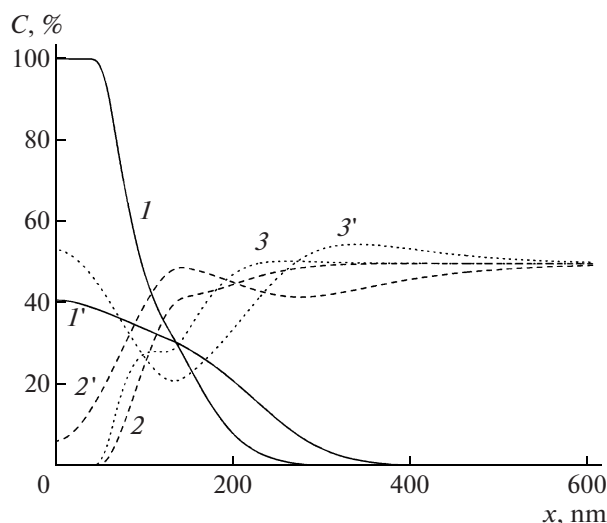


Fig. 3. Time effect of on the depth distribution of relative total concentrations C of metal (1, 1'), silicon (2, 2'), and free carbon (3, 3'). The calculation for $D_A = 6 \times 10^{-14}$ cm²/s, $k_{11} = k_{12} = 6 \times 10^{-26}$ cm³/s. The annealing time, min: (1–3)—10 and (1'–3')—60.

An increase in the rate constant for the silicide-formation reaction results in increasing the free-carbon accumulation in the front part of the reaction zone adjacent to the SiC substrate and to an ever increasing deviation of the ratio C_{CS}/C_{BS} of total concentrations of carbon and silicon from unity in this region.

The numerical solutions of the model were compared with the experimental distributions of the relative total concentrations of nickel, silicon, and carbon measured by the methods of secondary ion mass spectroscopy (SIMS) and the Auger electron spectroscopy combined with the ion etching of the Ni–SiC system formed at various annealing temperatures and under the conditions of proton irradiation.

In the SIMS method, we used the etching by positive Cs⁺ ions for equalizing the ion yields from metal and SiC, and the analysis was carried out with the complex ions CsNi⁺, CsSi⁺, and CsC⁺ according to the technique described in [24]. The annealing temperature amounted to $T = 850^\circ\text{C}$, the time of annealing was $t = 10$ min, and the Ni-film thickness was $h \approx 0.2$ μm. At this annealing temperature, silicide Ni₂Si enriched with metal [3, 7] prevails; therefore, we assumed in the calculation that $k_{12} = 0$ and $k_{21} = 10k_{11}$. In Fig. 4, the experimental profiles of total concentrations are compared with the calculated ones for the following values of parameters: $D_A = 1.1 \times 10^{-12}$ cm²/s and $k_{11} = 4 \times 10^{-25}$ cm³/s. To obtain satisfactory agreement with the experiment, we took into account the dependence of the metal diffusivity D_A on the composition of the type of Eq. (11) for the following relations between the partial diffusivities: $D_{BC} = 0.12D_A$ and $D_{AB} = D_{AAB} = 3.5D_A$.

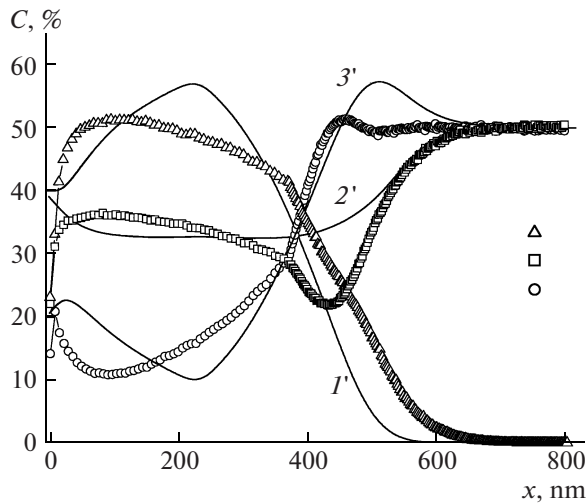


Fig. 4. (1–3) Experimental (SIMS) and (1'–3') calculated depth distributions of relative total concentrations C of (1, 1') metal, (2, 2') silicon, and (3, 3') carbon during the thermal annealing at $T = 850^\circ\text{C}$ for $t = 10$ min.

In [17], the samples of single-crystalline 6H-SiC with the nickel film of the thickness $h \approx 0.13 \mu\text{m}$ deposited on the surface were irradiated with protons with the energy $E = 40\text{--}100$ keV and the beam-current density $j = 5$ mA/cm² at the temperature $T = 750^\circ\text{C}$ for $t = 30$ min. The depth distribution of concentration of components was determined by the Auger method with etching by the Ar⁺-ion beam. In Fig. 5, we show the concentration profiles of components in the irradiation mode at the energy $E = 40$ keV with the path approximately corresponding to the nickel-film thickness ($R_p = 160$ nm). Under conditions of proton irradiation, the mixture of nickel monosilicide and disilicide (NiSi and NiSi₂) is formed [17]; therefore, we assumed in the calculations that $k_{11} = k_{12}$ and $k_{21} = 0$. Satisfactory agreement with the experiment is attained for the following values of parameters: $D_A = 1.5 \times 10^{-13}$ cm²/s, $k_{11} = 1 \times 10^{-25}$ cm³/s, $D_{BC} = 0.3D_A$, and $D_{AB} = D_{ABB} = 4D_A$. It should be noted that the found values of parameters exceed 2.5 and 10 times, respectively, the corresponding values for the control sample without the proton irradiation; i.e., the proton irradiation leads to a substantial increase in the metal diffusivities and the reaction-rate constants.

4. DISCUSSION OF RESULTS

As can be seen from Figs. 4 and 5, the results of experiments with the thermal annealing and the proton irradiation are well described within the framework of the suggested model on the basis of the diffusion of Ni in SiC instead of that of Si in Ni as it was assumed previously in [11, 13, 17]. The found Ni self-diffusivity proved to be 6.0×10^{-14} cm²/s at $T = 750^\circ\text{C}$ (without the proton irradiation) and 1.1×10^{-12} cm²/s at $T = 850^\circ\text{C}$, which approximately corresponds to the

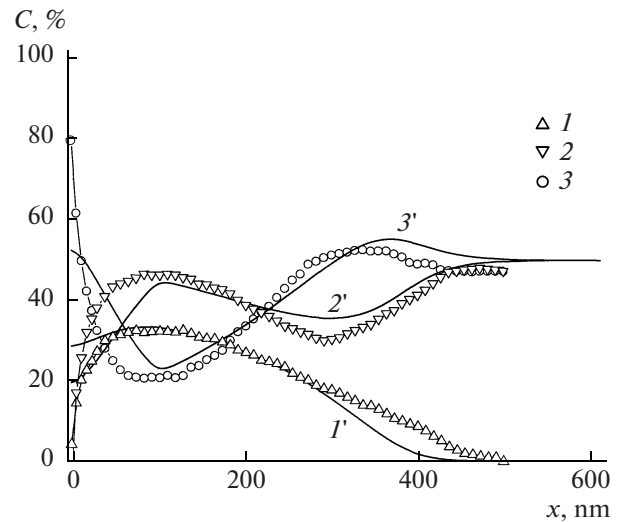


Fig. 5. (1–3) Experimental (Auger-spectroscopy [17]) and (1'–3') calculated depth distributions of relative total concentrations C of (1, 1') metal, (2, 2') silicon, and (3, 3') carbon under the proton irradiation ($E = 40$ keV, $j = 5$ mA/cm², $t = 30$ min) and at the increased temperature ($T = 750^\circ\text{C}$).

published data [25]. The Ni diffusivity proved to be 3.5–4 times higher in silicides and three–eight times lower in SiC than the Ni self-diffusivity. This result is also consistent with the published data showing that the Ni diffusivity in silicides is much higher than that in SiC [26, 27]. The deep penetration of Ni into the SiC substrate proves to be possible because of the low rate of silicide-formation reactions. Indeed, the estimate of the interaction radius R from the relation $k_{11} = 4\pi R D_A$ yields the value of $R \approx (3\text{--}5) \times 10^{-14}$ cm, which is many orders of magnitude smaller than the typical values of $(0.1\text{--}1) \times 10^{-8}$ cm for solid-state reactions between the components limited by diffusion. A low rate of reactions (1) and (2) of metal-silicide formation is caused, apparently, by the high strength of the Si–C bond and the necessity of removal of carbon reduced in reactions (1) and (3).

The difference in the total-concentration profiles of C and Si (in the SiC composition) in the front part of the reaction zone ($C_{CS}/C_{BS} > 1$) within the framework of the model is explained by pushing off free carbon reduced in reactions (1) and (3) by growing silicide phases towards the front part of the reaction zone. In the other (rear) part of the reaction zone, there is pushing off of free carbon to the surface. The carbon accumulation during the thermal annealing of the Ni/SiC system was observed previously experimentally at the internal interface between silicide and the SiC substrate [9, 10] and in the near-surface region [2, 6, 11–13]. We note that the proposed model does not quite adequately describe the free-carbon distribution near the surface. The experimental profiles show the more pronounced accumulation also in a thinner

surface silicide layer than that calculated (see Figs. 4, 5). The model gives no accumulation at all for carbon in the near-surface layer of incompletely reacted metal (compare curves 3 and 3' in Fig. 3). The carbon accumulation in a thin (~ 13 nm) near-surface Ni layer was observed experimentally even at the annealing temperature of 450°C of the Ni–SiC system [28]. The authors of [28] explained the effect by the diffusion of carbon released in the boundary silicide-formation reaction to the surface through a metal layer. This surface accumulation of carbon was retained even after the full transformation of the nickel film into that of silicide Ni_2Si , when the annealing temperature was elevated to 700°C [28]. In our model, the carbon diffusion through the metal layer to the surface was disregarded (it was assumed that $D_C = 0$).

The stimulation of metal diffusivity by the proton irradiation at increased temperatures is the consequence of the formation of elementary radiation defects (interstitial atoms and vacancies). These intrinsic point defects accelerate the metal diffusion in all available phases (the known effect of radiation-enhanced diffusion [29]).

For proceeding solid-phase reactions (1)–(3), the free volume is necessary because the molecular volumes of silicides $\{\Omega(\text{NiSi}) = 24.3 \text{ \AA}^3, \Omega(\text{Ni}_2\text{Si}) = 33.4 \text{ \AA}^3, \text{ and } \Omega(\text{NiSi}_2) = 39.5 \text{ \AA}^3 [30]\}$ exceeds the SiC molecular volume $\{\Omega(\text{SiC}) = 20.8 \text{ \AA}^3\}$. It is interesting to note that the formation of the nickel-disilicide phase with the highest molecular volume is observed only under conditions of the proton irradiation at the temperatures of 750 – 850°C [17], whereas the Ni_2Si phase [3–5, 7, 8], in which the molecular volume is smaller prevails during the usual thermal annealing with the temperatures of 600 – 950°C . Therefore, it is natural to relate the stimulation of solid-phase reactions (1)–(3) by proton irradiation, first of all, with the delivery of free volume by the vacancies formed under proton irradiation.

5. CONCLUSIONS

For the first time, the quantitative model of the interaction between the film of silicide-forming metal Ni and SiC, which is based on the mutual diffusion of components and the volume reactions of metal-silicide formation, was developed. The model enables us to describe well the basic properties of redistribution of components during the firing of Ni films into SiC, exactly, the large extent of the reaction zone, the excess of the carbon concentration over the silicon concentration in the front part of the reaction zone adjoining the SiC substrate, and the carbon accumulation near the surface. The found diffusivities of nickel in silicides are much higher than those in SiC, which corresponds to the published data. It is shown that the stimulation of the interaction between metal Ni and SiC by the proton irradiation at the elevated temperature occurs due to increasing the metal diffusivity and

the constants of rates of silicide-formation reactions. The acceleration of the metal diffusion is associated with the generation of elementary radiation defects (interstitial atoms and vacancies), whereas the increase in the constants of reaction rates with the generation of vacancies, which contribute the free volume for the solid-phase silicide-formation reactions.

ACKNOWLEDGMENTS

We thank Yu. Kudriavtsev and R. Asomoza (Department Ingenieria Electronica—SEES, CINVESTAV-IPN, Mexico) for carrying out the SIMS measurements, and also N.N. Afonin for the interest in the study and useful remarks.

REFERENCES

1. F. Roccaforte, F. La Via, and V. Raineri, *Int. J. High Speed Electron. Syst.* **15**, 781 (2005).
2. J. Crofton, L. M. Porter, and J. R. Williams, *Phys. Status Solidi B* **202**, 581 (1997).
3. C. S. Pai, C. M. Hanson, and S. S. Lau, *J. Appl. Phys.* **57**, 618 (1985).
4. I. Ohdomari, S. Sha, H. Aochi, and T. Chikyow, *J. Appl. Phys.* **62**, 3747 (1987).
5. J. Crofton, P. G. McMullin, J. R. Williams, and M. J. Bozack, *J. Appl. Phys.* **77**, 1317 (1995).
6. W. F. Slijberman, A. E. Fischer, J. F. van der Veen, I. Ohdomary, S. Yoshida, and S. Misawa, *J. Appl. Phys.* **66**, 666 (1989).
7. F. La Via and F. Roccaforte, *Microelectron. Eng.* **70**, 519 (2003).
8. F. Roccaforte, F. La Via, V. Raineri, L. Calcagno, and P. Musumeci, *Appl. Surf. Sci.* **184**, 295 (2001).
9. A. Kakanakova-Georgieva, T. Marinova, O. Noblanc, C. Arnodo, S. Cassette, and C. Brylinski, *Thin Sol. Films* **343–344**, 637 (1999).
10. I. P. Nikitina, K. V. Vassilevski, N. G. Wright, A. B. Horsfall, A. G. O'Neill, and C. M. Johnson, *J. Appl. Phys.* **97**, 083709 (2005).
11. E. Kurimoto, H. Harima, T. Toda, M. Sawada, M. Iwami, and S. Nakashima, *J. Appl. Phys.* **91**, 10215 (2002).
12. S. Y. Han, K. H. Kim, J. K. Kim, H. W. Jang, K. H. Lee, N.-K. Kim, E. D. Kim, and J.-L. Lee, *Appl. Phys. Lett.* **79**, 1816 (2001).
13. S. Y. Han and J.-L. Lee, *J. Electrochem. Soc.* **149**, G189 (2002).
14. L. Calcagno, E. Zanetti, F. La Via, and F. Roccaforte, *Mater. Sci. Forum* **433–436**, 721 (2003).
15. F. Roccaforte, L. Calcagno, P. Musumeci, and F. La Via, *Mater. Sci. Forum* **353–356**, 255 (2001).
16. V. V. Kozlovski, V. N. Lomasov, D. S. Rumyantsev, I. V. Grekhov, P. A. Ivanov, T. P. Samsonova, H. I. Helava, and L. O. Ragle, *Nucl. Instrum. Methods Phys. Res. B* **215**, 385 (2004).
17. V. V. Kozlovskii, P. A. Ivanov, D. S. Rumyantsev, V. N. Lomasov, and T. P. Samsonova, *Fiz. Tekh. Polu-*

- provodn. **38**, 778 (2004) [Semiconductors **38**, 745 (2004)].
18. A. D. Smigelskas and E. O. Kirkendall, Trans. AIME **171**, 130 (1947).
 19. L. S. Darken, Trans. AMIE **175**, 184 (1948).
 20. *Thin Films—Interdiffusion and Reactions*, Ed. by J. M. Poate, K. N. Tu, and J. W. Mayer (Wiley, New York, 1978; MIR, Moscow, 1982).
 21. B. A. Julies, D. Knoesen, R. Pretorius, and D. Adams, Thin Sol. Films **347**, 201 (1999).
 22. J. H. Güppen, A. A. Kodentsov, and F. J. J. van Loo, Z. Metallkd. **86**, 530 (1995).
 23. K. Bhanumurthy and R. Schmid-Fetzer, Composites A **32**, 569 (2001).
 24. Yu. Kudriavtsev, A. Villegas, A. Godines, and R. Asomoza, Appl. Surf. Sci. **206**, 187 (2003).
 25. M.-P. Macht, A. Müller, V. Naundorf, and H. Wollenberger, Nucl. Instrum. Methods Phys. Res. B **16**, 148 (1986).
 26. J. C. Ciccarello, S. Poize, and P. Gas, J. Appl. Phys. **67**, 3315 (1990).
 27. R. Nagel, K. Weyrich, D. H. H. Hofmann, and A. G. Balogh, Nucl. Instrum. Methods Phys. Res. B **178**, 315 (2001).
 28. A. Bächli, M.-A. Nicolet, L. Baud, C. Jaussaud, and R. Madar, Mater. Sci. Eng. B **56**, 11 (1998).
 29. V. V. Kozlovskii, *Modification of Semiconductors with Proton Beams* (Nauka, St.-Petersburg, 2003) [in Russian].
 30. S. P. Murarka, *Silicides for VLSI Applications* (Academic Press, New York, 1984).

Translated by V. Bukhanov